
1 **High secondary formation of nitrogen-containing organics (NOCs) and its**
2 **possible link to oxidized organics and ammonium**

3 Guohua Zhang¹, Xiufeng Lian^{1,2}, Yuzhen Fu^{1,2}, Qin hao Lin¹, Lei Li³, Wei Song¹, Zhanyong
4 Wang⁴, Mingjin Tang¹, Duohong Chen⁵, Xinhui Bi^{1,*}, Xinming Wang¹, Guoying Sheng¹

5

6 ¹State Key Laboratory of Organic Geochemistry and Guangdong Provincial Key Laboratory of
7 Environmental Protection and Resources Utilization, Guangzhou Institute of Geochemistry,
8 Chinese Academy of Sciences, Guangzhou 510640, PR China

9 ²University of Chinese Academy of Sciences, Beijing 100039, PR China

10 ³ Institute of Mass Spectrometry and Atmospheric Environment, Guangdong Provincial
11 Engineering Research Center for On-line Source Apportionment System of Air Pollution, Jinan
12 University, Guangzhou 510632, China

13 ⁴School of Intelligent Systems Engineering, Sun Yat-sen University, Shenzhen 518107, PR
14 China

15 ⁵ State Environmental Protection Key Laboratory of Regional Air Quality Monitoring,
16 Guangdong Environmental Monitoring Center, Guangzhou 510308, PR China

17

18 Correspondence to: Xinhui Bi (bixh@gig.ac.cn)

19

20 **Highlights**

- 21 ● Nitrogen-containing organics (NOCs) were highly internally mixed with photochemically
22 produced secondary oxidized organics
- 23 ● NOCs could be well predicted by the variations of these oxidized organics and ammonium
- 24 ● Higher relative humidity and NO_x may facilitate the conversion of these oxidized organics
25 to NOCs

26 **Abstract**

27 Nitrogen-containing organic compounds (NOCs) substantially contribute to light-
28 absorbing organic aerosols, although the atmospheric processes responsible for the secondary
29 formation of these compounds are poorly understood. In this study, seasonal atmospheric
30 processing of NOCs was investigated by single-particle mass spectrometry in urban Guangzhou
31 from 2013-2014. The relative abundance of NOCs is found to be strongly enhanced when
32 internally mixed with the photochemically produced secondary oxidized organics (i.e., formate,
33 acetate, pyruvate, methylglyoxal, glyoxylate, oxalate, malonate, and succinate) and ammonium.
34 Besides, both the hourly detected particle number and relative abundance of NOCs are highly
35 correlated with those of secondary oxidized organics and ammonium. It is therefore
36 hypothesized that secondary formation of NOCs most likely links to the oxidized organics and
37 ammonium. Results from both multiple linear regression analysis and positive matrix
38 factorization analysis further show that the relative abundance of NOCs could be well predicted
39 ($R^2 > 0.7$, $p < 0.01$) by the oxidized organics and ammonium.

40 Interestingly, the relative abundance of NOCs is inversely correlated with ammonium,
41 whereas their number fractions are positively correlated. This result suggests that although the
42 formation of NOCs does require the involvement of $\text{NH}_3/\text{NH}_4^+$, the relative amount of
43 ammonium may have a negative effect. Higher humidity and NO_x likely facilitate the
44 conversion of oxidized organics to NOCs. Due to the relatively high oxidized organics and
45 $\text{NH}_3/\text{NH}_4^+$, the relative contributions of NOCs in summer and autumn were higher than those in
46 spring and winter. To the best of our knowledge, this is the first direct field observation study

47 reporting a close association between NOCs and both oxidized organics and ammonium. These
48 findings have substantial implications for the role of ammonium in the atmosphere, particularly
49 in models that predict the evolution and deposition of NOCs.

50

51 **Keywords:** nitrogen-containing organic compounds, individual particles, oxidized organics,
52 ammonium, mixing state, single-particle mass spectrometry

54 **1 Introduction**

55 Organic aerosols that strongly absorb solar radiation are referred to as brown carbon
56 (BrC), capable of a comparable level of light absorption in the spectral range of near-
57 ultraviolet (UV) light as black carbon (Andreae and Gelencser, 2006; Feng et al., 2013; Yan
58 et al., 2018). Nitrogen-containing organic compounds (NOCs) substantially contribute to the
59 pool of BrC (Feng et al., 2013; Mohr et al., 2013; Li et al., 2019), and have a significant
60 effect on atmospheric chemistry, human health and climate forcing (Noziere et al., 2015;
61 Kanakidou et al., 2005; Shrivastava et al., 2017; De Gouw and Jimenez, 2009). The
62 particulate organic nitrogen accounts for a large fraction of total airborne nitrogen (~30%),
63 although the proportion exhibits a high variability temporally and spatially, and therefore
64 has an influence on both regional and global N deposition (Neff et al., 2002; Shi et al., 2010;
65 Cape et al., 2011). However, the sources, evolution, and optical properties of NOCs remain
66 unclear and contribute significantly to uncertainties in the estimation of their impacts on the
67 environment and climate (Laskin et al., 2015; Feng et al., 2013).

68 NOCs are ubiquitous components of atmospheric aerosols, cloud water and rainwater
69 (Altieri et al., 2009; Desyaterik et al., 2013; Laskin et al., 2015), spanning a wide range of
70 molecular weights, structures and light absorption properties (Lin et al., 2016). Emissions of
71 primary NOCs have been attributed to biomass burning, coal combustion, vehicle emissions,
72 biogenic production and soil dust (Laskin et al., 2009; Desyaterik et al., 2013; Sun et al.,
73 2017; Mace et al., 2003; Rastogi et al., 2011; Wang et al., 2017). A growing body of evidence

74 from laboratory studies suggests that secondary NOCs may be produced in gas phase,
75 aerosol, and clouds. Maillard reactions involving mixtures of atmospheric aldehydes (e.g.,
76 methylglyoxal/glyoxal) and ammonium/amines are of particular interest (e.g., Hawkins et
77 al., 2016; De Haan et al., 2017; De Haan et al., 2011). A significant portion of NOCs may
78 also be derived from the heterogeneous ageing of secondary organic aerosol (SOA) with
79 $\text{NH}_3 / \text{NH}_4^+$ (Liu et al., 2015; Laskin et al., 2015). Mang et al. (2008) proposed that even
80 trace levels of ammonia may be sufficient to form NOCs via this pathway. In addition, gas-
81 phase formation of NOCs through interaction between volatile organic hydrocarbons and
82 NO_x and other oxidations, followed by condensation, may have a potential contribution (Fry
83 et al., 2014; Lehtipalo et al., 2018).

84 The secondary formation of NOCs is especially prevalent in environments experiencing
85 high anthropogenic emissions (Yu et al., 2017; Ho et al., 2015), although further studies are
86 required to establish the formation mechanisms comprehensively. A major obstacle is that
87 organic and inorganic matrix effects have a profound impact on the chemistry of organic
88 compounds in bulk aqueous particles and particles undergoing drying (El-Sayed et al., 2015;
89 Lee et al., 2013). While real-time characterization studies remain a challenge due to the
90 extremely complex chemical nature of NOCs, establishing this data along with the co-
91 variation of NOCs with other chemical components would help to identify the sources and
92 evolution of NOCs. Using single-particle aerosol time-of-flight mass spectrometry, Wang et
93 al. (2010) observed that the widespread occurrence of NOCs closely correlated with particle
94 acidity in the atmosphere of Shanghai (China). In addition, real-time measurements of the

95 atmosphere in New York (US) by aerosol mass spectrometry indicated a definite link
96 between the age of organic species and the N/C ratio (Sun et al., 2011). Further in-depth
97 studies are required to identify the role of formation conditions (e.g., relative humidity (RH)
98 and pH) for secondary NOCs (Aiona et al., 2017; Nguyen et al., 2012). In the present study,
99 the mixing state of individual particles was investigated, involving NOCs, oxidized organics,
100 and ammonium, based on on-line seasonal observations using a single particle aerosol mass
101 spectrometry (SPAMS). Our findings show that the formation of NOCs is significantly
102 linked to oxidized organics and NH_4^+ , which has important environmental implications for
103 assessing the impact and fate of these compounds.

104

105 **2 Methods**

106 **2.1 Field measurements**

107 Sampling was constructed at the Guangzhou Institute of Geochemistry, a representative
108 urban site in Guangzhou (China), a megacity in the Pearl River Delta (PRD) region. The size
109 and chemical composition of individual particles were obtained by the SPAMS (Hexin
110 Analytical Instrument Co., Ltd., China) in real-time (Li et al., 2011). The sampling inlet for
111 aerosol characterization was situated 40 meters above the ground level. A brief description
112 of the performance of the SPAMS and other instruments can be found in the Supporting
113 Information. The sampling periods covered four seasons, including spring (21/02 to 11/04
114 2014), summer (13/06 to 16/07 2013), autumn (26/09 to 19/10 2013), and winter (15/12 to
115 25/12 2013). The total measured particle numbers and mean values for meteorological data

116 and gaseous pollutants, are outlined for each season in Table S1 and were described in a
117 previous publication (Zhang et al., 2019).

118

119 **2.2 SPAMS data analysis**

120 Fragments of NOCs were identified according to the detection of ion peaks at m/z -26
121 $[\text{CN}]^-$ or -42 $[\text{CNO}]^-$, generally due to the presence of C-N bonds (Silva and Prather, 2000;
122 Zawadowicz et al., 2017; Pagels et al., 2013). Laboratory produced C-N bonds compounds
123 from bulk solution-phase reactions between the representative oxidized organics (i.e.,
124 methylglyoxal) and ammonium sulfate was used to confirm the generation of ion peaks at
125 m/z -26 $[\text{CN}]^-$ and/or -42 $[\text{CNO}]^-$ using SPAMS (Fig. S1). Thus, the NOCs herein may refer
126 to complex nitrated organics such as organic nitrates, nitro-aromatics, nitrogen heterocycles,
127 and polyphenols. Unfortunately, how well $[\text{CN}]^- / [\text{CNO}]^-$ ions could represent NOCs cannot
128 be quantified, although they were the most commonly reported NOCs peaks by single-
129 particle mass spectrometry (Silva and Prather, 2000; Zawadowicz et al., 2017; Pagels et al.,
130 2013). In the present study, $[\text{CN}]^- / [\text{CNO}]^-$ ions are among the major peaks detected by the
131 SPAMS (Fig. 1). A rough estimate from the peak area ratio of $[\text{CN}]^- / [\text{CNO}]^-$ ions and the
132 most likely NOCs fragments (i.e., various amines, and an entire series of nitrogen-containing
133 cluster ions C_nN^- , $n = 1, 2, 3, \dots$) (Silva and Prather, 2000) shows that $[\text{CN}]^- / [\text{CNO}]^-$ ions
134 may represent more than 90% of these NOCs peaks. The number fractions (Nfs) of particles
135 that contained NOCs ranged from 56-59% across all four seasons (Table S1). The number
136 of detected NOCs-containing particles distributing along their vacuum aerodynamic

137 diameter (d_{va}) is shown in Fig. S2. Most of the detected NOC-containing particles had a d_{va}
138 in a range of 300-1200 nm.

139 A representative mass spectrum for NOCs-containing particles is shown in Fig. 1.
140 Dominant peaks in the mass spectrum were 39 [K]⁺, 23 [Na]⁺, nitrate (-62 [NO₃]⁻ or -46
141 [NO₂]⁻), sulfate (-97 [HSO₄]⁻), organics (27 [C₂H₃]⁺, 63 [C₅H₃]⁺, -42 [CNO]⁻, -26 [CN]⁻),
142 ammonium (18 [NH₄]⁺) and carbon ion clusters (C_n^{+/-}, n = 1, 2, 3,...). NOCs-containing
143 particles were internally mixed with various oxidized organics, represented as formate at m/z
144 -45 [HCO₂]⁻, acetate at m/z -59 [CH₃CO₂]⁻, methylglyoxal at m/z -71 [C₃H₃O₂]⁻, glyoxylate
145 at m/z -73 [C₂HO₃]⁻, pyruvate at m/z -87 [C₃H₃O₃]⁻, malonate at m/z -103 [C₃H₃O₄]⁻ and
146 succinate at m/z -117 [C₄H₅O₄]⁻ (Zhang et al., 2017; Zauscher et al., 2013; Lee et al., 2003).
147 These oxidized organics showed their pronounced diurnal trends with afternoon maximum
148 and were highly correlated ($r = 0.72 - 0.94$, $p < 0.01$) with each other. Therefore, they were
149 primarily attributed to secondary oxidized organics from photochemical oxidation products
150 of various volatile organic compounds (VOCs) (Paulot et al., 2011; Zhao et al., 2012; Ho et
151 al., 2011), and the details can be found in our previous publication (Zhang et al., 2019). More
152 information on the seasonal variation range of the Nfs of oxidized organics, ammonium and
153 NOCs is presented in Fig. S3.

154 Hourly mean Nfs and relative peak areas were applied herein to indicate the variations
155 of aerosol compositions in individual particles. Even though advances have been made in
156 the quantification of specific chemical species for individual particles based on their
157 respective peak area information, it is still quite a challenge for SPAMS to provide

158 quantitative information on aerosol components mainly due to matrix effects, incomplete
159 ionization and so forth (Qin et al., 2006; Jeong et al., 2011; Healy et al., 2013; Zhou et al.,
160 2016). Despite this, the variation of relative peak area should be a good indicator for the
161 investigation of atmospheric processing of various species in individual particles (Wang et
162 al., 2010; Zauscher et al., 2013; Sullivan and Prather, 2007; Zhang et al., 2014).

163

164 **3 Results and Discussion**

165 **3.1 Evidence for the formation of NOCs from oxidized organics and ammonium**

166 Figure 2 shows the seasonal variations in Nfs of the oxidized organics and ammonium,
167 which were internally mixed with NOCs. On average, more than 90% of the oxidized
168 organics and 65% of ammonium (except spring) were found to be internally mixed with
169 NOCs (Fig. S4). Regarding that the Nfs of NOCs relative to all the measured particles was
170 ~60%, it could be concluded that NOCs were enhanced with the presence of oxidized
171 organics and ammonium, with the enhancement associated with oxidized organics being the
172 most pronounced.

173 A strong correlation between both the Nfs and relative peak areas (RPAs) of NOCs and
174 oxidized organics further demonstrates their close associations, as shown in Fig. 3.
175 Compared with the oxidized organics, the Nfs of ammonium-containing particles internally
176 mixed with NOCs varied within a broader range (~40-90%). However, there is still an
177 enhancement mixing of NOCs with ammonium. A positive correlation ($R^2 = 0.50$, $p < 0.01$)
178 is observed between the hourly detected number of NOCs and ammonium. It is worth noting

179 that a negative correlation ($R^2 = 0.55$, $p < 0.01$) is obtained between the hourly average RPAs
180 of NOCs and ammonium (Fig. 3).

181 Based on both the enhancement of NOCs and the high correlations with oxidized
182 organics and ammonium, it is hypothesized that interactions between oxidized organics and
183 ammonium contributed to the observed NOCs. The formation of NOCs from ammonium
184 and carbonyls has been confirmed in several laboratory studies (Sareen et al., 2010; Shapiro
185 et al., 2009; Nozriere et al., 2009; Kampf et al., 2016; Galloway et al., 2009). Secondary
186 organic aerosols (SOA) produced from a large group of biogenic and anthropogenic VOCs
187 can be further aged by $\text{NH}_3/\text{NH}_4^+$ to generate NOCs (Nguyen et al., 2012; Bones et al., 2010;
188 Updyke et al., 2012; Liu et al., 2015; Huang et al., 2017). In a chamber study, the formation
189 of NOCs is enhanced in an NH_3 -rich environment (Chu et al., 2016). While such chemical
190 mechanisms might be complicated, the initial steps generally involve reactions forming
191 imines and amines, which can further react with carbonyl SOA compounds to form more
192 complex products (e.g., oligomers/BrC) (Laskin et al., 2015).

193 To verify this hypothesis, multiple linear regression analysis is performed to test how
194 well the RPAs of NOCs could be predicted by the oxidized organics and ammonium. As
195 expected, there is a close association ($R^2 = 0.71$, $p < 0.01$) between the predicted RPAs and
196 the observed values of NOCs (Fig. 4), which supports this hypothesis. A noticeable
197 improvement in R^2 implies that a model that uses both oxidized organics and ammonium to
198 predict RPAs of NOCs is substantially better than one that uses only one predictor (either
199 oxidized organics or ammonium in Fig. 3). The result indicates that interactions involving

200 oxidized organics and ammonium could explain over half of the observed variations in
201 NOCs in the atmosphere of Guangzhou. A fraction of the unaccounted NOCs could be due
202 to primary emissions and other formation pathways. This hypothesis could also be supported
203 by a similar pattern of diurnal variation observed for NOCs and oxidized organics (Fig. S5),
204 although there is a slight lag for the NOCs. Such a diurnal pattern is similar to those observed
205 in Beijing and Uintah (Yuan et al., 2016; Zhang et al., 2015). Notably, such a diurnal pattern
206 of secondary NOCs is adequately modelled when the production of NOCs via carbonyls and
207 ammonium is included (Woo et al., 2013). In addition to possible photo-bleaching (Zhao et
208 al., 2015), the lower contribution of NOCs during the daytime may be partly explained by
209 the lower RH, as discussed in section 3.2.

210 Interestingly, the relationship between NOCs and ammonium is distinctly different from
211 the relationship between NOCs and oxidized organics (Fig. 3). This implies that the
212 controlling factors on the formation of NOCs from ammonium are different from oxidized
213 organics. On the one hand, the positive correlation between the detected numbers reflects
214 that the formation of NOCs does require the participant of $\text{NH}_3/\text{NH}_4^+$, consistent with the
215 enhancement of NOCs in ammonium-containing particles (Fig. 2) discussed above. On the
216 other hand, the negative correlation between the RPAs signifies that the formation of NOCs
217 is most probably influenced by the relative amount of ammonium in individual particles.
218 Such influence could also be supported by our data, both from filter samples and individual
219 particle analysis. There is a negative correlation between concentrations of WSON and NH_4^+
220 for the filter samples (Fig. S6). It can be seen from Fig. S7 that lower RPAs of ammonium

221 correspond to higher Nfs of ammonium that internally mixed with NOCs. Such an inverse
222 correlation could also serve as evidence to explain the influence of the relative amount of
223 ammonium on the formation of NOCs.

224 The influence of relative ammonium amount on the formation of NOCs is also
225 theoretically possible since the formation of NOCs may be enhanced by particle acidity
226 (Miyazaki et al., 2014; Aiona et al., 2017; Nguyen et al., 2012), which is substantially
227 affected by the abundance of ammonium. Consistently, higher relative acidity was observed
228 for the internally mixed ammonium and NOCs particles, compared to ammonium-containing
229 particles without NOCs (Fig. S6) and thus may influence the formation of NOCs (Fig. S7).
230 Particle acidity could also play a significant role in the gas-to-particle partitioning of
231 aldehydes (Herrmann et al., 2015; Liggio et al., 2005; Gen et al., 2018; De Haan et al., 2018;
232 Kroll et al., 2005), precursors for the formation of oxidized organics. However, the higher
233 relative acidity might also be a result of NOCs formation. A model simulation shows that
234 after including the chemistry of SOA ageing with NH₃, an increase in aerosol acidity would
235 be expected due to the reduction in ammonium (Zhu et al., 2018). It is also noted that the
236 particle acidity is roughly estimated by the relative abundance of ammonium, nitrate, and
237 sulfate in individual particles (Denkenberger et al., 2007), and thus may not be representative
238 of actual aerosol acidity or pH (Guo et al., 2015; Hennigan et al., 2015; Murphy et al., 2017).
239 In addition, ammonia in the gas phase is also efficient at producing NOCs (Nguyen et al.,
240 2012), which may play an intricate role in the distribution of ammonium and NOCs in the
241 particulate phase. The formation of ammonium and NOCs would compete for ammonia,

242 which may also potentially result in the negative correlation between the RPAs of NOCs and
243 ammonium. Unfortunately, such a role remains unclear since the variations of ammonia were
244 not available in the present study.

245

246 **3.2 Factors contributing to the NOCs resolved by positive matrix factorization (PMF)** 247 **analysis**

248 Figure 5 presents the PMF factor profiles obtained from the PMF model analysis
249 (detailed information is provided in the SI) (Norris et al., 2009) and their diurnal variations.
250 Around 75% of NOCs could be well explained by two factors, with 33% of the PMF resolved
251 NOCs mainly associated with ammonium and carbonaceous ion peaks (ammonium factor),
252 while 59% were mainly associated with oxidized organics (oxidized organics factor). The
253 explained fraction of NOCs by the ammonium and oxidized organic factors is consistent
254 with the linear regression analysis. Furthermore, PMF analysis provided information on the
255 factor contribution and diurnal variations, which may help explain the seasonal variations
256 and processes of NOCs. The ammonium factor showed a diurnal variation pattern peaking
257 during the early morning, which is consistent with the diurnal variation in RH (Zhang et al.,
258 2019). This factor contributed to ~80% (Fig. S8) of the PMF resolved NOCs during spring
259 with the highest RH (Table S1), whereas the oxidized organics factor dominated (> 80%) in
260 summer and fall. In winter, these two factors similarly contributed (~40%). Variation of the
261 ammonium factor may reflect a potential role of aqueous pathways in the formation of NOCs,
262 particularly during spring. Differently, the oxidized organics factor showed a pattern of

263 diurnal variation, increasing from morning hours and peaking overnight, which may
264 correspond to the photochemical production of oxidized organics and followed interactions
265 with condensed ammonium. This pathway may explain the slightly late peaking of NOCs
266 compared to oxidized organics, as ammonium condensation is favorable overnight (Hu et al.,
267 2008). While there were similarities in the fractions of oxidized organics in the oxalate factor
268 and the oxidized organics factor, they only contributed to 8% of the PMF resolved NOCs in
269 the oxalate factor, which contained ~80% of the PMF resolved oxalate. As previously
270 discussed, these oxidized organics are also precursors for the formation of oxalate (Zhang et
271 al., 2019). Therefore, the PMF results suggest that there are two competitive pathways for
272 the evolution of these oxidized organics. Some oxidized organics formed from
273 photochemical activities were further oxidized to oxalate, resulting in a diurnal pattern of
274 variation with concentration peaks during the afternoon (Fig. 5), while others interact with
275 $\text{NH}_3/\text{NH}_4^+$ to form NOCs, peaking during the nighttime. However, the controlling factors for
276 these pathways could not be determined in the present study. The unexplained NOCs (~25%)
277 might be linked to the primary emissions, such as biomass burning (Desyaterik et al., 2013).
278 It could be partly supported by the presence of potassium and various carbon ion clusters (C
279 $_{n}^{+/-}$, $n = 1, 2, 3, \dots$) in the mass spectrum of NOCs-containing particles (Fig. 1).

280

281 **3.3 Seasonal variations in the observed NOCs**

282 There is an evident seasonal variation of NOCs, with higher relative contributions
283 during summer and autumn (Figs. 3 and 4), mainly due to the variations in oxidized organics

284 and $\text{NH}_3/\text{NH}_4^+$. In this region, a more considerable contribution from secondary oxidized
285 organics is typically observed during summer and autumn (Zhou et al., 2014; Yuan et al.,
286 2018). The seasonal maximum NH_3 concentrations have also been reported during the
287 warmer seasons, corresponding to the peak emissions from agricultural activities and high
288 temperatures, while the low NH_3 concentrations observed in colder seasons may be
289 attributed to gas-to-particle conversion (Pan et al., 2018; Zheng et al., 2012). Such seasonal
290 variation in NOCs is also obtained in a model simulation, showing that the conversion of
291 NH_3 into NOCs would result in a significantly higher reduction of gas-phase NH_3 during
292 summer (67%) than winter (31%), due to the higher NH_3 and SOA concentrations present in
293 the summer (Zhu et al., 2018). More primary NOCs may also be present during summer and
294 autumn in the present study, due to the additional biomass burning activities in these seasons
295 (Chen et al., 2018; Zhang et al., 2013).

296 The seasonal variations of NOCs can be adequately explained by the variations in
297 concentrations of oxidized organics and ammonium (Fig. 4), although the hourly variations
298 during each season are not well explained, as indicated by the lower R^2 values (Table S2).
299 The correlation coefficients (R^2) range from 0.24 to 0.57 for inter-seasonal variations.
300 During spring, NOCs exhibits a limited dependence on oxidized organics (Figs. 3a and 3b),
301 while during summer, the hourly detected number of NOCs shows a limited dependence on
302 ammonium (Fig. 3d). These seasonal dependences of NOCs are consistent with the PMF
303 results, showing that the ammonium factor explained ~80% of the predicted NOCs during

304 spring, while the oxidized organics factor dominantly contributed to the predicted NOCs
305 during warmer seasons (Fig. S8). A detailed discussion of this issue is provided in the SI.

306

307 **3.4 Influence of RH and NO_x**

308 The influence of RH on RPAs of NOCs and peak ratios of NOCs/oxidized organics are
309 shown in Fig. 6. While NOCs do not show a clear dependence on RH, the ratio of NOCs to
310 the oxidized organics shows an apparent increase towards higher RH. This finding is
311 consistent with the observations reported by Xu et al. (2017), in which the N/C ratio
312 significantly increases as a function of RH in the atmosphere of Beijing. Besides, the diurnal
313 variations of NOCs with peaks values around 20:00 are also similar to those reported by Xu
314 et al. (2017). The peak ratios of NOCs/oxidized organics are more obviously enhanced when
315 RH is higher than 40%. These findings imply that aqueous-phase processing likely plays a
316 substantial role in the formation of NOCs. Significant changes in RH, such as during the
317 evaporation of water droplets, have been reported to facilitate the formation of NOCs via
318 NH₃/NH₄⁺ and SOA (Nguyen et al., 2012). In addition, an increase in RH would improve
319 the uptake of NH₃ and the formation of NH₄⁺, which also contributes to the enhancement of
320 NOCs. However, the relatively weak correlation ($R^2 = 0.27$, $p < 0.01$) between the peak
321 ratios and RH, reflect the complex influence of RH on the formation of NOCs (Xu et al.,
322 2017; Woo et al., 2013).

323 One may expect that NOCs are formed through the interactions between NO_x and
324 oxidized organics in the gas phase, followed by condensation (Fry et al., 2014; Lehtipalo et

325 al., 2018). Similar to that observed for RH, while NOCs do not show a clear dependence on
326 NO_x (Fig. 6c, $R^2 = 0.02\text{--}0.13$), the ratio of NOCs to the oxidized organics shows a clear
327 increasing trend towards higher NO_x (Fig. 6d, $R^2 = 0.18$, $p < 0.01$). This indicates that NO_x
328 may play a certain role in the conversion of oxidized organics to NOCs, and yet it cannot be
329 quantified in the present study. It is also noted that low correlation coefficients between NO_x
330 and NOCs might not indicate a limited contribution of NO_x to the formation of NOCs. NO_x
331 affects the formation of NOCs in various ways (e.g., peroxy radical chemistry in VOCs
332 oxidation mechanisms and formation of nitrate radicals) {Xu, 2015 #20234}{Zhang, 2018
333 #22855}, and thus may not linearly contribute to the formation of NOCs.

334

335 **3.5 Atmospheric implications and limitation**

336 In this study, we showed that in an urban megacity area, secondary NOCs were
337 significantly contributed by the heterogeneous ageing of oxidized organics with NH₃/NH₄⁺,
338 providing valuable insight into SOA aging mechanisms. In particular, the effects of NH₃/NH
339 ⁺ on SOA or BrC formation remain relatively poorly understood. In the PRD region, it has
340 been shown that oxygenated organic aerosols (OOA) account for more than 40% of the total
341 organic mass (He et al., 2011), with high concentrations of available gaseous carbonyls (Li
342 et al., 2014). Therefore, it is expected that over half of all water-soluble NOCs in this region
343 might link to secondary processing (Yu et al., 2017). Furthermore, secondary sources have
344 been found to contribute significantly to NOCs related BrC in Nanjing, China (Chen et al.,
345 2018). The results presented herein also suggest that the production of NOCs might be

346 adequately estimated by their correlation with secondary oxidized organics and ammonium.
347 The effectiveness of correlation-based estimations needs to be examined in other regions
348 before being generally applied in other environments. However, this approach may provide
349 valuable insights into investigations of NOCs using atmospheric observations. In contrast, it
350 has previously been reported that a positive correlation exists between WSON and
351 ammonium (Li et al., 2012), indicating similar anthropogenic sources. This divergence could
352 be mainly attributed to varying contributions of primary sources and secondary processes to
353 the observed NOCs. Possible future reductions in anthropogenic emissions of ammonia may
354 reduce particle NOCs. Understanding the complex interplay between inorganic and organic
355 nitrogen is an essential part of assessing global nitrogen cycling.

356 Moise et al. (2015) proposed that with high concentrations of reduced nitrogen
357 compounds, high photochemical activity, and frequent changes in humidity, BrC formed via
358 $\text{NH}_3/\text{NH}_4^+$ and SOA may become a dominant contributor to aerosol absorption, specifically
359 in agricultural and forested areas. However, this study suggests that even in typical urban
360 areas, BrC formation via $\text{NH}_3/\text{NH}_4^+$ and SOA should not be neglected. In particular, SOA
361 was found to account for 44 – 71% of the organic mass in megacities across China (Huang
362 et al., 2014), with NH_3 concentrations in urban areas comparable with those from agricultural
363 sites and 2- or 3-fold those of forested areas in China (Pan et al., 2018). Additionally, the
364 acidic nature of particles in these regions would also be favorable for the formation of NOCs
365 (Guo et al., 2017; Jia et al., 2018). Considering the formation of NOCs from the uptake of

366 NH₃ onto SOA particles, Zhu et al. (2018) suggested that this mechanism could have a
367 significant impact on the atmospheric concentrations of NH₃/NH₄⁺ and NO₃.

368

369 **5 Conclusions**

370 This study investigated the processes contributing to the seasonal formation of NOCs,
371 involving ammonium and oxidized organics in urban Guangzhou, using single-particle mass
372 spectrometry. This is the first study to provide direct field observation results to confirm that
373 the variation of NOCs correlate well and are strongly enhanced internal mixing with
374 secondary oxidized organics. These findings highlight the possible formation pathway of
375 NOCs through the ageing of secondary oxidized organics by NH₃/NH₄⁺ in ambient urban
376 environments. A clear pattern of seasonal variation in NOCs was observed, with higher
377 relative contributions in summer and autumn as compared to spring and winter. This
378 seasonal variation was well predicted by multiple linear regression model analysis, using the
379 relative abundance of oxidized organics and ammonium as model inputs. More than 50% of
380 NOCs could be explained by the interaction between oxidized organics and ammonium. The
381 production of NOCs through such processes was facilitated by increased humidity and NO_x.
382 These results extend our understanding of the mixing state and atmospheric processing of
383 particulate NOCs, as well as having substantial implications for the accuracy of models
384 predicting the formation, fate, and impacts of NOCs in the atmosphere.

385

386 **Author contribution**

387 GHZ and XHB designed the research (with input from WS, LL, ZYW, DHC, MJT, XMW
388 and GYS), analyzed the data, and wrote the manuscript. XFL, YZF, and QHL conducted air
389 sampling work and laboratory experiments under the guidance of GHZ, XHB and XMW.
390 All authors contributed to the refinement of the submitted manuscript.

391

392 **Acknowledgement**

393 This work was supported by the National Nature Science Foundation of China (No.
394 41775124 and 41877307), the National Key Research and Development Program of China
395 (2017YFC0210104 and 2016YFC0202204), the Science and Technology Project of
396 Guangzhou, China (No. 201803030032), and the Guangdong Foundation for Program of
397 Science and Technology Research (No. 2017B030314057).

398 **References**

399 Aiona, P. K., Lee, H. J., Leslie, R., Lin, P., Laskin, A., Laskin, J., and Nizkorodov, S. A.:
400 Photochemistry of Products of the Aqueous Reaction of Methylglyoxal with Ammonium
401 Sulfate, *Acs Earth Space Chem.*, 1, 522-532, doi:10.1021/acsearthspacechem.7b00075, 2017.

402 Altieri, K. E., Turpin, B. J., and Seitzinger, S. P.: Composition of Dissolved Organic
403 Nitrogen in Continental Precipitation Investigated by Ultra-High Resolution FT-ICR Mass
404 Spectrometry, *Environ. Sci. Technol.*, 43, 6950-6955, doi:10.1021/es9007849, 2009.

405 Andreae, M. O., and Gelencser, A.: Black carbon or brown carbon? The nature of light-
406 absorbing carbonaceous aerosols, *Atmos. Chem. Phys.*, 6, 3131-3148, 2006.

407 Bones, D. L., Henricksen, D. K., Mang, S. A., Gonsior, M., Bateman, A. P., Nguyen, T.
408 B., Cooper, W. J., and Nizkorodov, S. A.: Appearance of strong absorbers and fluorophores in
409 limonene-O-3 secondary organic aerosol due to NH₄⁺-mediated chemical aging over long time
410 scales, *J. Geophys. Res.-Atmos.*, 115, D05203, doi:10.1029/2009jd012864, 2010.

411 Cape, J. N., Cornell, S. E., Jickells, T. D., and Nemitz, E.: Organic nitrogen in the
412 atmosphere — Where does it come from? A review of sources and methods, *Atmos. Res.*, 102,
413 30-48, doi:10.1016/j.atmosres.2011.07.009, 2011.

414 Chen, Y., Ge, X., Chen, H., Xie, X., Chen, Y., Wang, J., Ye, Z., Bao, M., Zhang, Y., and
415 Chen, M.: Seasonal light absorption properties of water-soluble brown carbon in atmospheric
416 fine particles in Nanjing, China, *Atmos. Environ.*,
417 doi:<https://doi.org/10.1016/j.atmosenv.2018.06.002>, 2018.

418 Chu, B. W., Zhang, X., Liu, Y. C., He, H., Sun, Y., Jiang, J. K., Li, J. H., and Hao, J. M.:
419 Synergetic formation of secondary inorganic and organic aerosol: effect of SO₂ and NH₃ on
420 particle formation and growth, *Atmos. Chem. Phys.*, 16, 14219-14230, doi:10.5194/acp-16-
421 14219-2016, 2016.

422 De Gouw, J., and Jimenez, J. L.: Organic Aerosols in the Earth's Atmosphere, *Environ.*
423 *Sci. Technol.*, 43, 7614-7618, doi:10.1021/Es9006004, 2009.

424 De Haan, D. O., Hawkins, L. N., Kononenko, J. A., Turley, J. J., Corrigan, A. L., Tolbert,
425 M. A., and Jimenez, J. L.: Formation of Nitrogen-Containing Oligomers by Methylglyoxal and

426 Amines in Simulated Evaporating Cloud Droplets, *Environ. Sci. Technol.*, 45, 984-991,
427 doi:10.1021/es102933x, 2011.

428 De Haan, D. O., Hawkins, L. N., Welsh, H. G., Pednekar, R., Casar, J. R., Pennington, E.
429 A., de Loera, A., Jimenez, N. G., Symons, M. A., Zauscher, M., Pajunoja, A., Caponi, L.,
430 Cazaunau, M., Formenti, P., Gratien, A., Pangui, E., and Doussin, J.-F.: Brown Carbon
431 Production in Ammonium- or Amine-Containing Aerosol Particles by Reactive Uptake of
432 Methylglyoxal and Photolytic Cloud Cycling, *Environ. Sci. Technol.*, 51, 7458-7466,
433 doi:10.1021/acs.est.7b00159, 2017.

434 De Haan, D. O., Jimenez, N. G., de Loera, A., Cazaunau, M., Gratien, A., Pangui, E., and
435 Doussin, J.-F.: Methylglyoxal Uptake Coefficients on Aqueous Aerosol Surfaces, *J. Phys.*
436 *Chem. A*, 122, 4854-4860, doi:10.1021/acs.jpca.8b00533, 2018.

437 Denkenberger, K. A., Moffet, R. C., Holecek, J. C., Rebotier, T. P., and Prather, K. A.:
438 Real-time, single-particle measurements of oligomers in aged ambient aerosol particles,
439 *Environ. Sci. Technol.*, 41, 5439-5446, doi:10.1021/es070329l, 2007.

440 Desyaterik, Y., Sun, Y., Shen, X., Lee, T., Wang, X., Wang, T., and Collett, J. L., Jr.:
441 Speciation of "brown" carbon in cloud water impacted by agricultural biomass burning in
442 eastern China, *J. Geophys. Res.-Atmos.*, 118, 7389-7399, doi:10.1002/jgrd.50561, 2013.

443 El-Sayed, M. M. H., Wang, Y. Q., and Hennigan, C. J.: Direct atmospheric evidence for
444 the irreversible formation of aqueous secondary organic aerosol, *Geophys. Res. Lett.*, 42, 5577-
445 5586, doi:10.1002/2015gl064556, 2015.

446 Feng, Y., Ramanathan, V., and Kotamarthi, V. R.: Brown carbon: a significant
447 atmospheric absorber of solar radiation?, *Atmos. Chem. Phys.*, 13, 8607-8621,
448 doi:10.5194/acp-13-8607-2013, 2013.

449 Fry, J. L., Draper, D. C., Barsanti, K. C., Smith, J. N., Ortega, J., Winkle, P. M., Lawler,
450 M. J., Brown, S. S., Edwards, P. M., Cohen, R. C., and Lee, L.: Secondary Organic Aerosol
451 Formation and Organic Nitrate Yield from NO₃ Oxidation of Biogenic Hydrocarbons, *Environ.*
452 *Sci. Technol.*, 48, 11944-11953, doi:10.1021/es502204x, 2014.

453 Galloway, M. M., Chhabra, P. S., Chan, A. W. H., Surratt, J. D., Flagan, R. C., Seinfeld,
454 J. H., and Keutsch, F. N.: Glyoxal uptake on ammonium sulphate seed aerosol: reaction
455 products and reversibility of uptake under dark and irradiated conditions, *Atmos. Chem. Phys.*,
456 9, 3331-3345, doi:10.5194/acp-9-3331-2009, 2009.

457 Gen, M., Huang, D. D., and Chan, C. K.: Reactive Uptake of Glyoxal by Ammonium-
458 Containing Salt Particles as a Function of Relative Humidity, *Environ. Sci. Technol.*, 52, 6903-
459 6911, doi:10.1021/acs.est.8b00606, 2018.

460 Guo, H., Xu, L., Bougiatioti, A., Cerully, K. M., Capps, S. L., Hite, J. R., Carlton, A. G.,
461 Lee, S. H., Bergin, M. H., Ng, N. L., Nenes, A., and Weber, R. J.: Fine-particle water and pH
462 in the southeastern United States, *Atmos. Chem. Phys.*, 15, 5211-5228, doi:10.5194/acp-15-
463 5211-2015, 2015.

464 Guo, H., Weber, R. J., and Nenes, A.: High levels of ammonia do not raise fine particle
465 pH sufficiently to yield nitrogen oxide-dominated sulfate production, *Sci. Rep.*, 7, 12109,
466 doi:10.1038/s41598-017-11704-0, 2017.

467 Hawkins, L. N., Lemire, A. N., Galloway, M. M., Corrigan, A. L., Turley, J. J., Espelien,
468 B. M., and De Haan, D. O.: Maillard Chemistry in Clouds and Aqueous Aerosol As a Source
469 of Atmospheric Humic-Like Substances, *Environ. Sci. Technol.*, 50, 7443-7452,
470 doi:10.1021/acs.est.6b00909, 2016.

471 He, L. Y., Huang, X. F., Xue, L., Hu, M., Lin, Y., Zheng, J., Zhang, R. Y., and Zhang, Y.
472 H.: Submicron aerosol analysis and organic source apportionment in an urban atmosphere in
473 Pearl River Delta of China using high-resolution aerosol mass spectrometry, *J. Geophys. Res.-*
474 *Atmos.*, 116, 1-15, doi:10.1029/2010jd014566, 2011.

475 Healy, R. M., Sciare, J., Poulain, L., Crippa, M., Wiedensohler, A., Prevot, A. S. H.,
476 Baltensperger, U., Sarda-Estevé, R., McGuire, M. L., Jeong, C. H., McGillicuddy, E., O'Connor,
477 I. P., Sodeau, J. R., Evans, G. J., and Wenger, J. C.: Quantitative determination of carbonaceous
478 particle mixing state in Paris using single-particle mass spectrometer and aerosol mass
479 spectrometer measurements, *Atmos. Chem. Phys.*, 13, 9479-9496, doi:10.5194/acp-13-9479-
480 2013, 2013.

481 Hennigan, C. J., Izumi, J., Sullivan, A. P., Weber, R. J., and Nenes, A.: A critical
482 evaluation of proxy methods used to estimate the acidity of atmospheric particles, *Atmos. Chem.*
483 *Phys.*, 15, 2775-2790, doi:10.5194/acp-15-2775-2015, 2015.

484 Herrmann, H., Schaefer, T., Tilgner, A., Styler, S. A., Weller, C., Teich, M., and Otto, T.:
485 Tropospheric Aqueous-Phase Chemistry: Kinetics, Mechanisms, and Its Coupling to a
486 Changing Gas Phase, *Chem. Rev.*, 115, 4259-4334, doi:10.1021/cr500447k, 2015.

487 Ho, K. F., Ho, S. S. H., Lee, S. C., Kawamura, K., Zou, S. C., Cao, J. J., and Xu, H. M.:
488 Summer and winter variations of dicarboxylic acids, fatty acids and benzoic acid in PM_{2.5} in
489 Pearl Delta River Region, China, *Atmos. Chem. Phys.*, 11, 2197-2208, doi:10.5194/acp-11-
490 2197-2011, 2011.

491 Ho, K. F., Ho, S. S. H., Huang, R. J., Liu, S. X., Cao, J. J., Zhang, T., Chuang, H. C., Chan,
492 C. S., Hu, D., and Tian, L. W.: Characteristics of water-soluble organic nitrogen in fine
493 particulate matter in the continental area of China, *Atmos. Environ.*, 106, 252-261,
494 doi:10.1016/j.atmosenv.2015.02.010, 2015.

495 Hu, M., Wu, Z., Slanina, J., Lin, P., Liu, S., and Zeng, L.: Acidic gases, ammonia and
496 water-soluble ions in PM_{2.5} at a coastal site in the Pearl River Delta, China, *Atmos. Environ.*,
497 42, 6310-6320, 2008.

498 Huang, M., Xu, J., Cai, S., Liu, X., Zhao, W., Hu, C., Gu, X., Fang, L., and Zhang, W.:
499 Characterization of brown carbon constituents of benzene secondary organic aerosol aged with
500 ammonia, *J. Atmos. Chem.*, 75, 205-218, doi:10.1007/s10874-017-9372-x, 2017.

501 Huang, R. J., Zhang, Y., Bozzetti, C., Ho, K. F., Cao, J. J., Han, Y., Daellenbach, K. R.,
502 Slowik, J. G., Platt, S. M., Canonaco, F., Zotter, P., Wolf, R., Pieber, S. M., Bruns, E. A., Crippa,
503 M., Ciarelli, G., Piazzalunga, A., Schwikowski, M., Abbaszade, G., Schnelle-Kreis, J.,
504 Zimmermann, R., An, Z., Szidat, S., Baltensperger, U., El Haddad, I., and Prevot, A. S.: High
505 secondary aerosol contribution to particulate pollution during haze events in China, *Nature*, 514,
506 218-222, doi:10.1038/nature13774, 2014.

507 Jeong, C. H., McGuire, M. L., Godri, K. J., Slowik, J. G., Rehbein, P. J. G., and Evans, G.
508 J.: Quantification of aerosol chemical composition using continuous single particle
509 measurements, *Atmos. Chem. Phys.*, 11, 7027-7044, doi:10.5194/acp-11-7027-2011, 2011.

510 Jia, S. G., Sarkar, S., Zhang, Q., Wang, X. M., Wu, L. L., Chen, W. H., Huang, M. J.,
511 Zhou, S. Z., Zhang, J. P., Yuan, L., and Yang, L. M.: Characterization of diurnal variations of
512 PM_{2.5} acidity using an open thermodynamic system: A case study of Guangzhou, China,
513 *Chemosphere*, 202, 677-685, doi:10.1016/j.chemosphere.2018.03.127, 2018.

514 Kampf, C. J., Filippi, A., Zuth, C., Hoffmann, T., and Opatz, T.: Secondary brown carbon
515 formation via the dicarbonyl imine pathway: nitrogen heterocycle formation and synergistic
516 effects, *Phys. Chem. Chem. Phys.*, 18, 18353-18364, doi:10.1039/c6cp03029g, 2016.

517 Kanakidou, M., Seinfeld, J. H., Pandis, S. N., Barnes, I., Dentener, F. J., Facchini, M. C.,
518 Van Dingenen, R., Ervens, B., Nenes, A., Nielsen, C. J., Swietlicki, E., Putaud, J. P., Balkanski,
519 Y., Fuzzi, S., Horth, J., Moortgat, G. K., Winterhalter, R., Myhre, C. E. L., Tsigaridis, K.,
520 Vignati, E., Stephanou, E. G., and Wilson, J.: Organic aerosol and global climate modelling: a
521 review, *Atmos. Chem. Phys.*, 5, 1053-1123, 2005.

522 Kroll, J. H., Ng, N. L., Murphy, S. M., Varutbangkul, V., Flagan, R. C., and Seinfeld, J.
523 H.: Chamber studies of secondary organic aerosol growth by reactive uptake of simple carbonyl
524 compounds, *J. Geophys. Res.-Atmos.*, 110, doi:10.1029/2005JD006004, 2005.

525 Laskin, A., Smith, J. S., and Laskin, J.: Molecular Characterization of Nitrogen-
526 Containing Organic Compounds in Biomass Burning Aerosols Using High-Resolution Mass
527 Spectrometry, *Environ. Sci. Technol.*, 43, 3764-3771, doi:10.1021/es803456n, 2009.

528 Laskin, A., Laskin, J., and Nizkorodov, S. A.: Chemistry of Atmospheric Brown Carbon,
529 *Chem. Rev.*, 115, 4335-4382, doi:10.1021/cr5006167, 2015.

530 Lee, A. K. Y., Zhao, R., Li, R., Liggio, J., Li, S. M., and Abbatt, J. P. D.: Formation of
531 Light Absorbing Organo-Nitrogen Species from Evaporation of Droplets Containing Glyoxal
532 and Ammonium Sulfate, *Environ. Sci. Technol.*, 47, 12819-12826, doi:10.1021/es402687w,
533 2013.

534 Lee, S. H., Murphy, D. M., Thomson, D. S., and Middlebrook, A. M.: Nitrate and oxidized
535 organic ions in single particle mass spectra during the 1999 Atlanta Supersite Project, *J.*
536 *Geophys. Res.*, 108, 8417, doi:10.1029/2001jd001455, 2003.

537 Lehtipalo, K., Yan, C., Dada, L., Bianchi, F., Xiao, M., Wagner, R., Stolzenburg, D.,
538 Ahonen, L. R., Amorim, A., Baccharini, A., Bauer, P. S., Baumgartner, B., Bergen, A.,
539 Bernhammer, A.-K., Breitenlechner, M., Brilke, S., Buchholz, A., Mazon, S. B., Chen, D., Chen,
540 X., Dias, A., Dommen, J., Draper, D. C., Duplissy, J., Ehn, M., Finkenzeller, H., Fischer, L.,
541 Frege, C., Fuchs, C., Garmash, O., Gordon, H., Hakala, J., He, X., Heikkinen, L., Heinritzi, M.,
542 Helm, J. C., Hofbauer, V., Hoyle, C. R., Jokinen, T., Kangasluoma, J., Kerminen, V.-M., Kim,
543 C., Kirkby, J., Kontkanen, J., Kürten, A., Lawler, M. J., Mai, H., Mathot, S., Mauldin, R. L.,
544 Molteni, U., Nichman, L., Nie, W., Nieminen, T., Ojdanic, A., Onnela, A., Passananti, M.,
545 Petäjä, T., Piel, F., Pospisilova, V., Quéléver, L. L. J., Rissanen, M. P., Rose, C., Sarnela, N.,
546 Schallhart, S., Schuchmann, S., Sengupta, K., Simon, M., Sipilä, M., Tauber, C., Tomé, A.,
547 Tröstl, J., Väisänen, O., Vogel, A. L., Volkamer, R., Wagner, A. C., Wang, M., Weitz, L.,
548 Wimmer, D., Ye, P., Ylisirniö, A., Zha, Q., Carslaw, K. S., Curtius, J., Donahue, N. M., Flagan,
549 R. C., Hansel, A., Riipinen, I., Virtanen, A., Winkler, P. M., Baltensperger, U., Kulmala, M.,
550 and Worsnop, D. R.: Multicomponent new particle formation from sulfuric acid, ammonia, and
551 biogenic vapors, *Sci. Adv.*, 4, eaau5363, doi:10.1126/sciadv.aau5363, 2018.

552 Li, J., Fang, Y. T., Yoh, M., Wang, X. M., Wu, Z. Y., Kuang, Y. W., and Wen, D. Z.:
553 Organic nitrogen deposition in precipitation in metropolitan Guangzhou city of southern China,
554 *Atmos. Res.*, 113, 57-67, doi:10.1016/j.atmosres.2012.04.019, 2012.

555 Li, L., Huang, Z. X., Dong, J. G., Li, M., Gao, W., Nian, H. Q., Fu, Z., Zhang, G. H., Bi,
556 X. H., Cheng, P., and Zhou, Z.: Real time bipolar time-of-flight mass spectrometer for analyzing
557 single aerosol particles, *Intl. J. Mass. Spectrom.*, 303, 118-124, doi:10.1016/j.ijms.2011.01.017,
558 2011.

559 Li, X., Rohrer, F., Brauers, T., Hofzumahaus, A., Lu, K., Shao, M., Zhang, Y. H., and
560 Wahner, A.: Modeling of HCHO and CHOCHO at a semi-rural site in southern China during

561 the PRIDE-PRD2006 campaign, *Atmos. Chem. Phys.*, 14, 12291-12305, doi:10.5194/acp-14-
562 12291-2014, 2014.

563 Li, Z. J., Nizkorodov, S. A., Chen, H., Lu, X. H., Yang, X., and Chen, J. M.: Nitrogen-
564 containing secondary organic aerosol formation by acrolein reaction with ammonia/ammonium,
565 *Atmos. Chem. Phys.*, 19, 1343-1356, doi:10.5194/acp-19-1343-2019, 2019.

566 Liggio, J., Li, S. M., and McLaren, R.: Reactive uptake of glyoxal by particulate matter, *J.*
567 *Geophys. Res.-Atmos.*, 110, doi:10.1029/2004jd005113, 2005.

568 Lin, P., Aiona, P. K., Li, Y., Shiraiwa, M., Laskin, J., Nizkorodov, S. A., and Laskin, A.:
569 Molecular Characterization of Brown Carbon in Biomass Burning Aerosol Particles, *Environ.*
570 *Sci. Technol.*, 50, 11815-11824, doi:10.1021/acs.est.6603024, 2016.

571 Liu, Y., Liggio, J., Staebler, R., and Li, S. M.: Reactive uptake of ammonia to secondary
572 organic aerosols: kinetics of organonitrogen formation, *Atmos. Chem. Phys.*, 15, 13569-13584,
573 doi:10.5194/acp-15-13569-2015, 2015.

574 Mace, K. A., Kubilay, N., and Duce, R. A.: Organic nitrogen in rain and aerosol in the
575 eastern Mediterranean atmosphere: An association with atmospheric dust, *J. Geophys. Res.-*
576 *Atmos.*, 108, doi:10.1029/2002jd002997, 2003.

577 Mang, S. A., Henricksen, D. K., Bateman, A. P., Andersen, M. P. S., Blake, D. R., and
578 Nizkorodov, S. A.: Contribution of Carbonyl Photochemistry to Aging of Atmospheric
579 Secondary Organic Aerosol, *J. Phys. Chem. A*, 112, 8337-8344, doi:10.1021/jp804376c, 2008.

580 Miyazaki, Y., Fu, P. Q., Ono, K., Tachibana, E., and Kawamura, K.: Seasonal cycles of
581 water-soluble organic nitrogen aerosols in a deciduous broadleaf forest in northern Japan, *J.*
582 *Geophys. Res.-Atmos.*, 119, 1440-1454, doi:10.1002/2013JD020713, 2014.

583 Mohr, C., Lopez-Hilfiker, F. D., Zotter, P., Prévôt, A. S. H., Xu, L., Ng, N. L., Herndon,
584 S. C., Williams, L. R., Franklin, J. P., Zahniser, M. S., Worsnop, D. R., Knighton, W. B., Aiken,
585 A. C., Gorkowski, K. J., Dubey, M. K., Allan, J. D., and Thornton, J. A.: Contribution of
586 Nitrated Phenols to Wood Burning Brown Carbon Light Absorption in Detling, United
587 Kingdom during Winter Time, *Environ. Sci. Technol.*, 47, 6316-6324, doi:10.1021/es400683v,
588 2013.

589 Moise, T., Flores, J. M., and Rudich, Y.: Optical Properties of Secondary Organic Aerosols
590 and Their Changes by Chemical Processes, *Chem. Rev.*, 115, 4400-4439,
591 doi:10.1021/cr5005259, 2015.

592 Murphy, J. G., Gregoire, P. K., Tevlin, A. G., Wentworth, G. R., Ellis, R. A., Markovic,
593 M. Z., and VandenBoer, T. C.: Observational constraints on particle acidity using
594 measurements and modelling of particles and gases, *Faraday Discuss.*, 200, 379-395,
595 doi:10.1039/c7fd00086c, 2017.

596 Neff, J. C., Holland, E. A., Dentener, F. J., McDowell, W. H., and Russell, K. M.: The
597 origin, composition and rates of organic nitrogen deposition: A missing piece of the nitrogen
598 cycle?, *Biogeochemistry*, 57, 99-136, 2002.

599 Nguyen, T. B., Lee, P. B., Updyke, K. M., Bones, D. L., Laskin, J., Laskin, A., and
600 Nizkorodov, S. A.: Formation of nitrogen- and sulfur-containing light-absorbing compounds
601 accelerated by evaporation of water from secondary organic aerosols, *J. Geophys. Res.-Atmos.*,
602 117, D01207, doi:10.1029/2011jd016944, 2012.

603 Norris, G., Vedantham, R., Wade, K., Zahn, P., Brown, S., Paatero, P., Eberly, S., and
604 Foley, C. (2009), Guidance document for PMF applications with the Multilinear Engine, edited,
605 Prepared for the U.S. Environmental Protection Agency, Research Triangle Park, NC.

606 Noziere, B., Dziedzic, P., and Cordova, A.: Products and Kinetics of the Liquid-Phase
607 Reaction of Glyoxal Catalyzed by Ammonium Ions (NH₄⁺), *J. Phys. Chem. A*, 113, 231-237,
608 doi:10.1021/jp8078293, 2009.

609 Noziere, B., Kaberer, M., Claeys, M., Allan, J., D'Anna, B., Decesari, S., Finessi, E.,
610 Glasius, M., Grgic, I., Hamilton, J. F., Hoffmann, T., Iinuma, Y., Jaoui, M., Kahno, A., Kampf,
611 C. J., Kourtchev, I., Maenhaut, W., Marsden, N., Saarikoski, S., Schnelle-Kreis, J., Surratt, J.
612 D., Szidat, S., Szmigielski, R., and Wisthaler, A.: The Molecular Identification of Organic
613 Compounds in the Atmosphere: State of the Art and Challenges, *Chem. Rev.*, 115, 3919-3983,
614 doi:10.1021/cr5003485, 2015.

615 Pagels, J., Dutcher, D. D., Stolzenburg, M. R., McMurry, P. H., Galli, M. E., and Gross,
616 D. S.: Fine-particle emissions from solid biofuel combustion studied with single-particle mass

617 spectrometry: Identification of markers for organics, soot, and ash components, *J. Geophys.*
618 *Res.-Atmos.*, 118, 859-870, doi:10.1029/2012jd018389, 2013.

619 Pan, Y. P., Tian, S. L., Zhao, Y. H., Zhang, L., Zhu, X. Y., Gao, J., Huang, W., Zhou, Y.
620 B., Song, Y., Zhang, Q., and Wang, Y. S.: Identifying Ammonia Hotspots in China Using a
621 National Observation Network, *Environ. Sci. Technol.*, 52, 3926-3934,
622 doi:10.1021/acs.est.7b05235, 2018.

623 Paulot, F., Wunch, D., Crouse, J. D., Toon, G. C., Millet, D. B., DeCarlo, P. F.,
624 Vigouroux, C., Deutscher, N. M., González Abad, G., Notholt, J., Warneke, T., Hannigan, J.
625 W., Warneke, C., de Gouw, J. A., Dunlea, E. J., De Mazière, M., Griffith, D. W. T., Bernath,
626 P., Jimenez, J. L., and Wennberg, P. O.: Importance of secondary sources in the atmospheric
627 budgets of formic and acetic acids, *Atmos. Chem. Phys.*, 11, 1989-2013, doi:10.5194/acp-11-
628 1989-2011, 2011.

629 Qin, X. Y., Bhave, P. V., and Prather, K. A.: Comparison of two methods for obtaining
630 quantitative mass concentrations from aerosol time-of-flight mass spectrometry measurements,
631 *Anal. Chem.*, 78, 6169-6178, doi:10.1021/ac060395q, 2006.

632 Rastogi, N., Zhang, X., Edgerton, E. S., Ingall, E., and Weber, R. J.: Filterable water-
633 soluble organic nitrogen in fine particles over the southeastern USA during summer, *Atmos.*
634 *Environ.*, 45, 6040-6047, doi:10.1016/j.atmosenv.2011.07.045, 2011.

635 Sareen, N., Schwier, A. N., Shapiro, E. L., Mitroo, D., and McNeill, V. F.: Secondary
636 organic material formed by methylglyoxal in aqueous aerosol mimics, *Atmos. Chem. Phys.*, 10,
637 997-1016, doi:10.5194/acp-10-997-2010, 2010.

638 Shapiro, E. L., Szprengiel, J., Sareen, N., Jen, C. N., Giordano, M. R., and McNeill, V. F.:
639 Light-absorbing secondary organic material formed by glyoxal in aqueous aerosol mimics,
640 *Atmos. Chem. Phys.*, 9, 2289-2300, 2009.

641 Shi, J., Gao, H., Qi, J., Zhang, J., and Yao, X.: Sources, compositions, and distributions of
642 water-soluble organic nitrogen in aerosols over the China Sea, *J. Geophys. Res.-Atmos.*, 115,
643 doi:10.1029/2009jd013238, 2010.

644 Shrivastava, M., Cappa, C. D., Fan, J. W., Goldstein, A. H., Guenther, A. B., Jimenez, J.
645 L., Kuang, C., Laskin, A., Martin, S. T., Ng, N. L., Petaja, T., Pierce, J. R., Rasch, P. J., Roldin,
646 P., Seinfeld, J. H., Shilling, J., Smith, J. N., Thornton, J. A., Volkamer, R., Wang, J., Worsnop,
647 D. R., Zaveri, R. A., Zelenyuk, A., and Zhang, Q.: Recent advances in understanding secondary
648 organic aerosol: Implications for global climate forcing, *Rev. Geophys.*, *55*, 509-559,
649 doi:10.1002/2016RG000540, 2017.

650 Silva, P. J., and Prather, K. A.: Interpretation of mass spectra from organic compounds in
651 aerosol time-of-flight mass spectrometry, *Anal. Chem.*, *72*, 3553-3562, 2000.

652 Stefenelli, G., Pospisilova, V., Lopez-Hilfiker, F. D., Daellenbach, K. R., Hüglin, C., Tong,
653 Y., Baltensperger, U., Prevot, A. S. H., and Slowik, J. G.: Organic aerosol source apportionment
654 in Zurich using extractive electrospray ionization time-of-flight mass spectrometry (EESI-TOF):
655 Part I, biogenic influences and day/night chemistry in summer, *Atmos. Chem. Phys. Discuss.*,
656 2019, 1-36, doi:10.5194/acp-2019-361, 2019.

657 Sullivan, R. C., and Prather, K. A.: Investigations of the diurnal cycle and mixing state of
658 oxalic acid in individual particles in Asian aerosol outflow, *Environ. Sci. Technol.*, *41*, 8062-
659 8069, 2007.

660 Sun, J. Z., Zhi, G. R., Hitzenberger, R., Chen, Y. J., Tian, C. G., Zhang, Y. Y., Feng, Y.
661 L., Cheng, M. M., Zhang, Y. Z., Cai, J., Chen, F., Qiu, Y., Jiang, Z., Li, J., Zhang, G., and Mo,
662 Y.: Emission factors and light absorption properties of brown carbon from household coal
663 combustion in China, *Atmos. Chem. Phys.*, *17*, 4769-4780, doi:10.5194/acp-17-4769-2017,
664 2017.

665 Sun, Y. L., Zhang, Q., Schwab, J. J., Demerjian, K. L., Chen, W. N., Bae, M. S., Hung, H.
666 M., Hogrefe, O., Frank, B., Rattigan, O. V., and Lin, Y. C.: Characterization of the sources and
667 processes of organic and inorganic aerosols in New York city with a high-resolution time-of-
668 flight aerosol mass spectrometer, *Atmos. Chem. Phys.*, *11*, 1581-1602, doi:10.5194/acp-11-
669 1581-2011, 2011.

670 Updyke, K. M., Nguyen, T. B., and Nizkorodov, S. A.: Formation of brown carbon via
671 reactions of ammonia with secondary organic aerosols from biogenic and anthropogenic
672 precursors, *Atmos. Environ.*, 63, 22-31, doi:10.1016/j.atmosenv.2012.09.012, 2012.

673 Wang, X. F., Gao, S., Yang, X., Chen, H., Chen, J. M., Zhuang, G. S., Surratt, J. D., Chan,
674 M. N., and Seinfeld, J. H.: Evidence for High Molecular Weight Nitrogen-Containing Organic
675 Salts in Urban Aerosols, *Environ. Sci. Technol.*, 44, 4441-4446, 2010.

676 Wang, X. F., Wang, H. L., Jing, H., Wang, W. N., Cui, W. D., Williams, B. J., and Biswas,
677 P.: Formation of Nitrogen-Containing Organic Aerosol during Combustion of High-Sulfur-
678 Content Coal, *Energ. Fuel.*, 31, 14161-14168, doi:10.1021/acs.energyfuels.7b02273, 2017.

679 Woo, J. L., Kim, D. D., Schwier, A. N., Li, R. Z., and McNeill, V. F.: Aqueous aerosol
680 SOA formation: impact on aerosol physical properties, *Faraday Discuss.*, 165, 357-367,
681 doi:10.1039/c3fd00032j, 2013.

682 Xu, L., Guo, H. Y., Boyd, C. M., Klein, M., Bougiatioti, A., Cerully, K. M., Hite, J. R.,
683 Isaacman-VanWertz, G., Kreisberg, N. M., Knote, C., Olson, K., Koss, A., Goldstein, A. H.,
684 Hering, S. V., de Gouw, J., Baumann, K., Lee, S. H., Nenes, A., Weber, R. J., and Ng, N. L.:
685 Effects of anthropogenic emissions on aerosol formation from isoprene and monoterpenes in
686 the southeastern United States, *Proc. Natl. Acad. Sci. USA*, 112, E4509-E4509,
687 doi:10.1073/pnas.1512279112, 2015.

688 Xu, W. Q., Sun, Y. L., Wang, Q. Q., Du, W., Zhao, J., Ge, X. L., Han, T. T., Zhang, Y. J.,
689 Zhou, W., Li, J., Fu, P. Q., Wang, Z. F., and Worsnop, D. R.: Seasonal Characterization of
690 Organic Nitrogen in Atmospheric Aerosols Using High Resolution Aerosol Mass Spectrometry
691 in Beijing, China, *Acs Earth Space Chem.*, 1, 673-682,
692 doi:10.1021/acsearthspacechem.7b00106, 2017.

693 Yan, J., Wang, X., Gong, P., Wang, C., and Cong, Z.: Review of brown carbon aerosols:
694 Recent progress and perspectives, *Sci. Total. Environ.*, 634, 1475-1485,
695 doi:<https://doi.org/10.1016/j.scitotenv.2018.04.083>, 2018.

696 Yu, X., Yu, Q. Q., Zhu, M., Tang, M. J., Li, S., Yang, W. Q., Zhang, Y. L., Deng, W., Li,
697 G. H., Yu, Y. G., Huang, Z. H., Song, W., Ding, X., Hu, Q. H., Li, J., Bi, X. H., and Wang, X.

698 M.: Water Soluble Organic Nitrogen (WSO_N) in Ambient Fine Particles Over a Megacity in
699 South China: Spatiotemporal Variations and Source Apportionment, *J. Geophys. Res.-Atmos.*,
700 122, 13045-13060, doi:10.1002/2017JD027327, 2017.

701 Yuan, B., Liggio, J., Wentzell, J., Li, S. M., Stark, H., Roberts, J. M., Gilman, J., Lerner,
702 B., Warneke, C., Li, R., Leithead, A., Osthoff, H. D., Wild, R., Brown, S. S., and de Gouw, J.
703 A.: Secondary formation of nitrated phenols: insights from observations during the Uintah
704 Basin Winter Ozone Study (UBWOS) 2014, *Atmos. Chem. Phys.*, 16, 2139-2153,
705 doi:10.5194/acp-16-2139-2016, 2016.

706 Yuan, Q., Lai, S., Song, J., Ding, X., Zheng, L., Wang, X., Zhao, Y., Zheng, J., Yue, D.,
707 Zhong, L., Niu, X., and Zhang, Y.: Seasonal cycles of secondary organic aerosol tracers in rural
708 Guangzhou, Southern China: The importance of atmospheric oxidants, *Environ. Pollut.*, 240,
709 884-893, doi:10.1016/j.envpol.2018.05.009, 2018.

710 Zauscher, M. D., Wang, Y., Moore, M. J. K., Gaston, C. J., and Prather, K. A.: Air Quality
711 Impact and Physicochemical Aging of Biomass Burning Aerosols during the 2007 San Diego
712 Wildfires, *Environ. Sci. Technol.*, 47, 7633-7643, doi:10.1021/es4004137, 2013.

713 Zawadowicz, M. A., Froyd, K. D., Murphy, D. M., and Cziczo, D. J.: Improved
714 identification of primary biological aerosol particles using single-particle mass spectrometry,
715 *Atmos. Chem. Phys.*, 17, 7193-7212, doi:10.5194/acp-17-7193-2017, 2017.

716 Zhang, G., Lin, Q., Peng, L., Yang, Y., Jiang, F., Liu, F., Song, W., Chen, D., Cai, Z., Bi,
717 X., Miller, M., Tang, M., Huang, W., Wang, X., Peng, P., and Sheng, G.: Oxalate Formation
718 Enhanced by Fe-Containing Particles and Environmental Implications, *Environ. Sci. Technol.*,
719 53, 1269-1277, doi:10.1021/acs.est.8b05280, 2019.

720 Zhang, G. H., Bi, X. H., He, J. J., Chen, D. H., Chan, L. Y., Xie, G. W., Wang, X. M.,
721 Sheng, G. Y., Fu, J. M., and Zhou, Z.: Variation of secondary coatings associated with
722 elemental carbon by single particle analysis, *Atmos. Environ.*, 92, 162-170,
723 doi:10.1016/j.atmosenv.2014.04.018, 2014.

724 Zhang, G. H., Lin, Q. H., Peng, L., Yang, Y. X., Fu, Y. Z., Bi, X. H., Li, M., Chen, D. H.,
725 Chen, J. X., Cai, Z., Wang, X. M., Peng, P. A., Sheng, G. Y., and Zhou, Z.: Insight into the in-

726 cloud formation of oxalate based on in situ measurement by single particle mass spectrometry,
727 *Atmos. Chem. Phys.*, 17, 13891-13901, doi:10.5194/acp-17-13891-2017, 2017.

728 Zhang, Q., Duan, F., He, K., Ma, Y., Li, H., Kimoto, T., and Zheng, A.: Organic nitrogen
729 in PM_{2.5} in Beijing, *Frontiers of Environmental Science & Engineering*, 9, 1004-1014,
730 doi:10.1007/s11783-015-0799-5, 2015.

731 Zhang, Y. S., Shao, M., Lin, Y., Luan, S. J., Mao, N., Chen, W. T., and Wang, M.:
732 Emission inventory of carbonaceous pollutants from biomass burning in the Pearl River Delta
733 Region, China, *Atmos. Environ.*, 76, 189-199, doi:10.1016/j.atmosenv.2012.05.055, 2013.

734 Zhao, R., Lee, A. K. Y., and Abbatt, J. P. D.: Investigation of Aqueous-Phase
735 Photooxidation of Glyoxal and Methylglyoxal by Aerosol Chemical Ionization Mass
736 Spectrometry: Observation of Hydroxyhydroperoxide Formation, *J. Phys. Chem. A*, 116, 6253-
737 6263, doi:10.1021/jp211528d, 2012.

738 Zhao, R., Lee, A. K. Y., Huang, L., Li, X., Yang, F., and Abbatt, J. P. D.: Photochemical
739 processing of aqueous atmospheric brown carbon, *Atmos. Chem. Phys.*, 15, 6087-6100,
740 doi:10.5194/acp-15-6087-2015, 2015.

741 Zheng, J. Y., Yin, S. S., Kang, D. W., Che, W. W., and Zhong, L. J.: Development and
742 uncertainty analysis of a high-resolution NH₃ emissions inventory and its implications with
743 precipitation over the Pearl River Delta region, China, *Atmos. Chem. Phys.*, 12, 7041-7058,
744 doi:10.5194/acp-12-7041-2012, 2012.

745 Zhou, S. Z., Wang, T., Wang, Z., Li, W. J., Xu, Z., Wang, X. F., Yuan, C., Poon, C. N.,
746 Louie, P. K. K., Luk, C. W. Y., and Wang, W. X.: Photochemical evolution of organic aerosols
747 observed in urban plumes from Hong Kong and the Pearl River Delta of China, *Atmos. Environ.*,
748 88, 219-229, doi:10.1016/j.atmosenv.2014.01.032, 2014.

749 Zhou, Y., Huang, X. H. H., Griffith, S. M., Li, M., Li, L., Zhou, Z., Wu, C., Meng, J. W.,
750 Chan, C. K., Louie, P. K. K., and Yu, J. Z.: A field measurement based scaling approach for
751 quantification of major ions, organic carbon, and elemental carbon using a single particle
752 aerosol mass spectrometer, *Atmos. Environ.*, 143, 300-312,
753 doi:10.1016/j.atmosenv.2016.08.054, 2016.

754 Zhu, S. P., Horne, J. R., Montoya-Aguilera, J., Hinks, M. L., Nizkorodov, S. A., and
755 Dabdub, D.: Modeling reactive ammonia uptake by secondary organic aerosol in CMAQ:
756 application to the continental US, *Atmos. Chem. Phys.*, 18, 3641-3657, doi:10.5194/acp-18-
757 3641-2018, 2018.

758

759 **Figure captions**

760 Figure 1. Representative mass spectrum for NOCs-containing particles. The ion
761 peaks corresponding to NOCs and oxidized organics are highlighted with red bars.

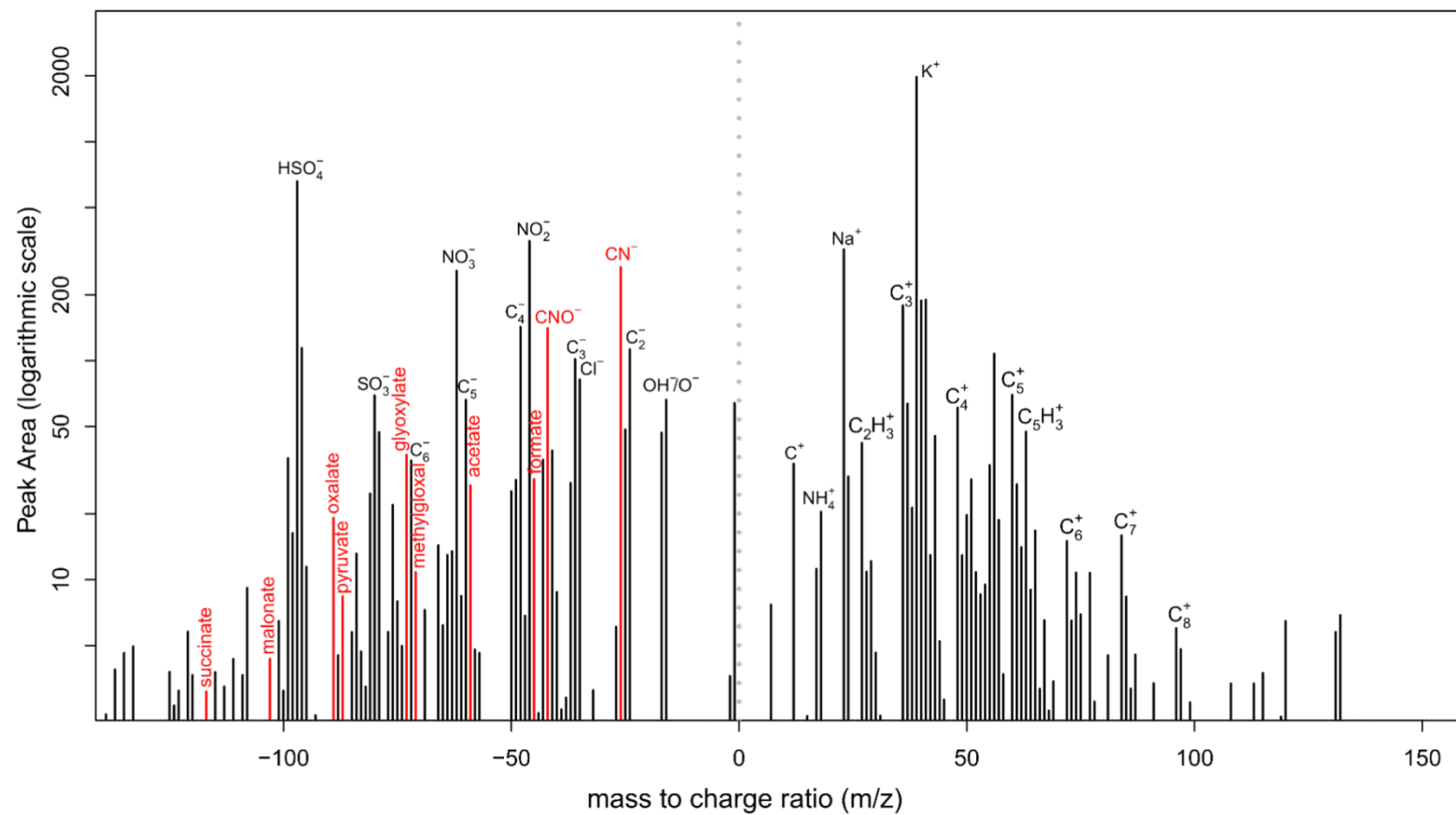
762 Figure 2. The variation in hourly mean Nfs of the oxidized organics and
763 ammonium that internally mixed with NOCs. Box and whisker plot shows lower,
764 median, and upper lines, denoting the 25th, 50th, and 75th percentiles, respectively; the
765 lower and upper edges denote the 10th and 90th percentiles, respectively.

766 Figure 3. Correlation analysis of (a, c) the RPAs and (b, d) the number of
767 detected NOCs, with the oxidized organics and ammonium in different seasons.
768 Significant ($p < 0.01$) correlations were obtained for both the total observed data and
769 the seasonally separated data. RPA is defined as the fractional peak area of each m/z
770 relative to the sum of peak areas in the mass spectrum and is applied to represent the
771 relative amount of a species on a particle (Jeong et al., 2011; Healy et al., 2013).

772 Figure 4. Comparison between the measured and predicted RPAs for NOCs.

773 Figure 5. (left) PMF-resolved 3-factor source profiles (percentage of total species)
774 and (right) their diurnal variations (arbitrary unit).

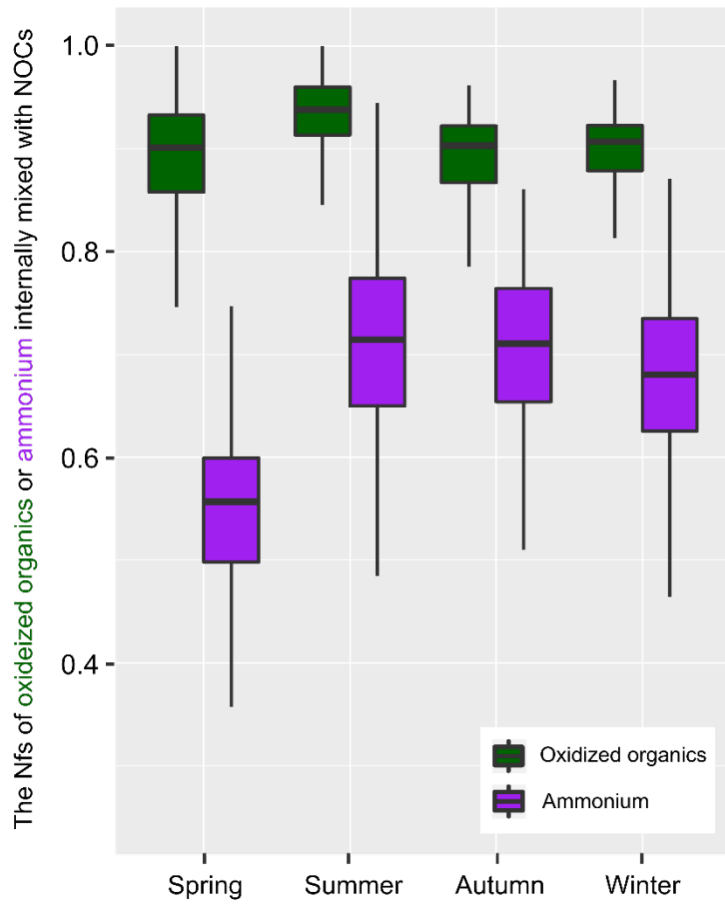
775 Figure 6. The dependence of NOCs and the ratio of NOCs to the oxidized organics
776 on RH.



777

778

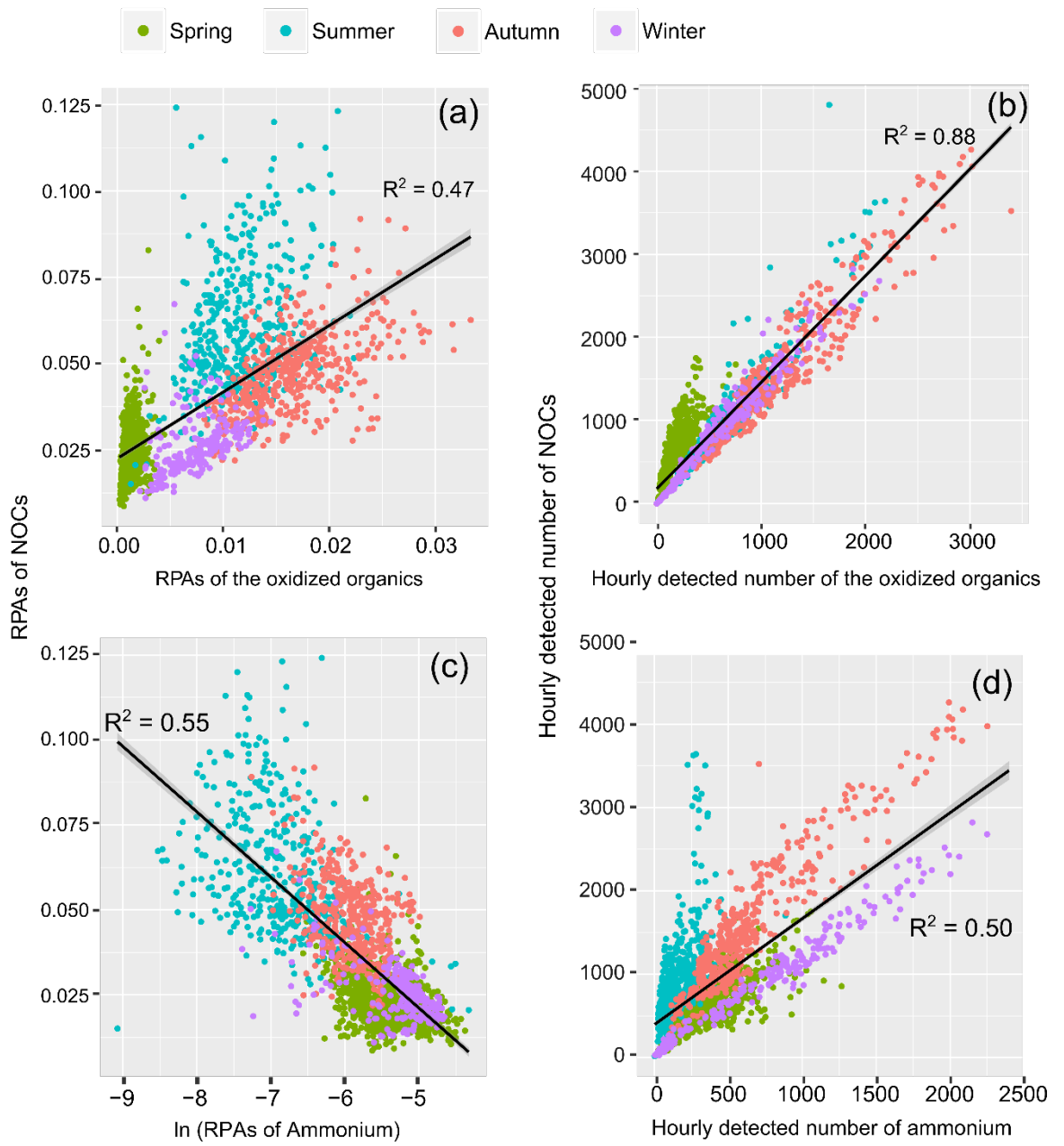
Fig. 1.



779

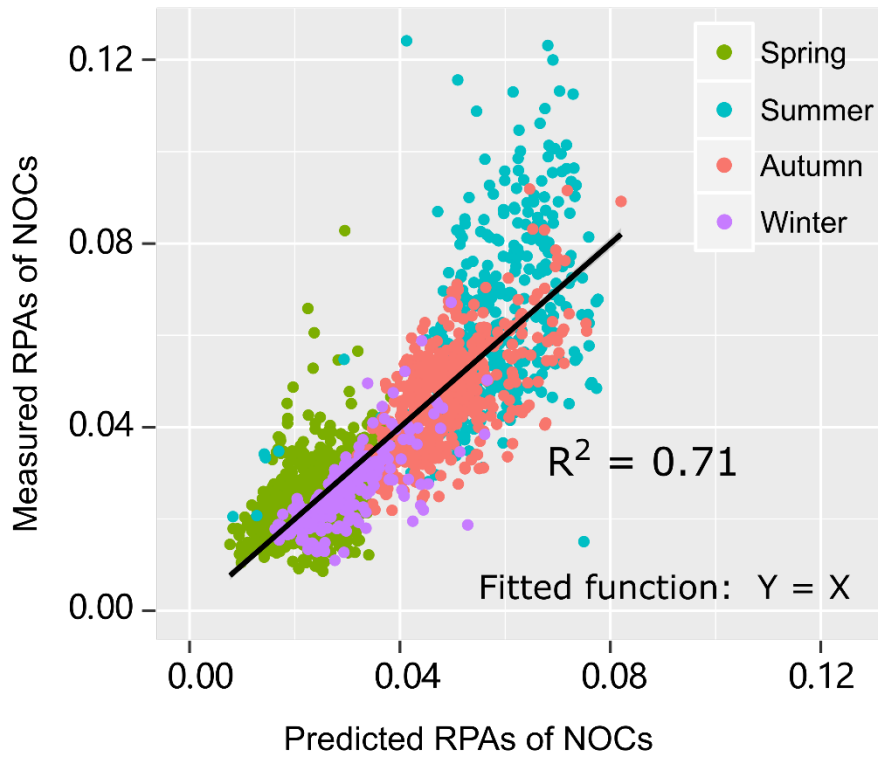
780

Fig. 2.



781

782 Fig. 3.

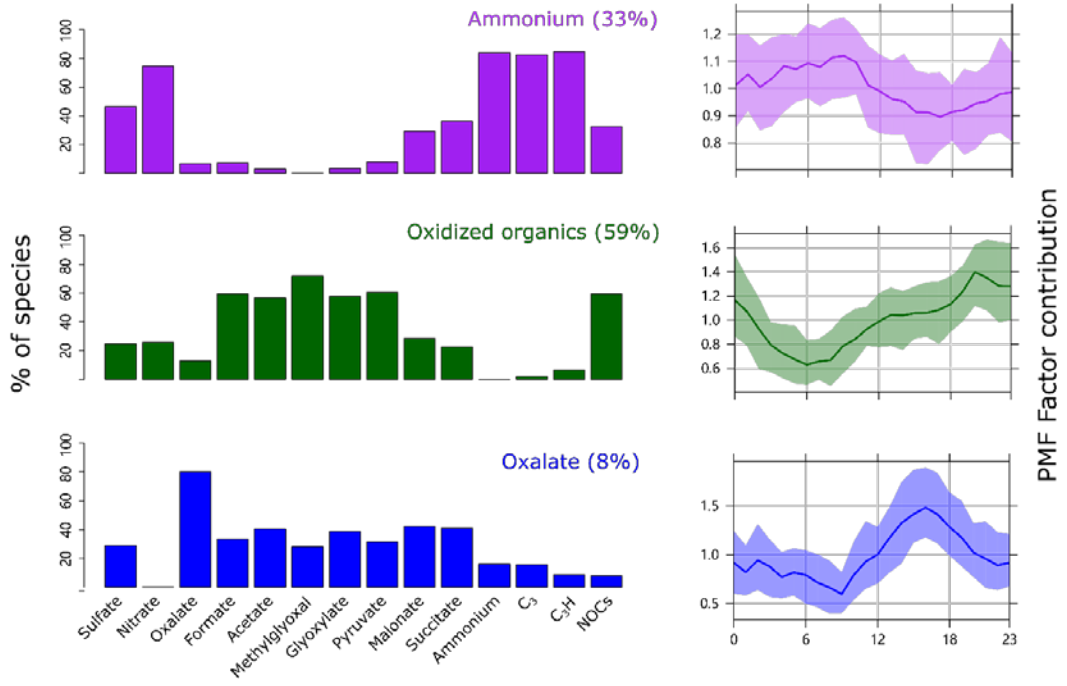


783

784

Fig. 4.

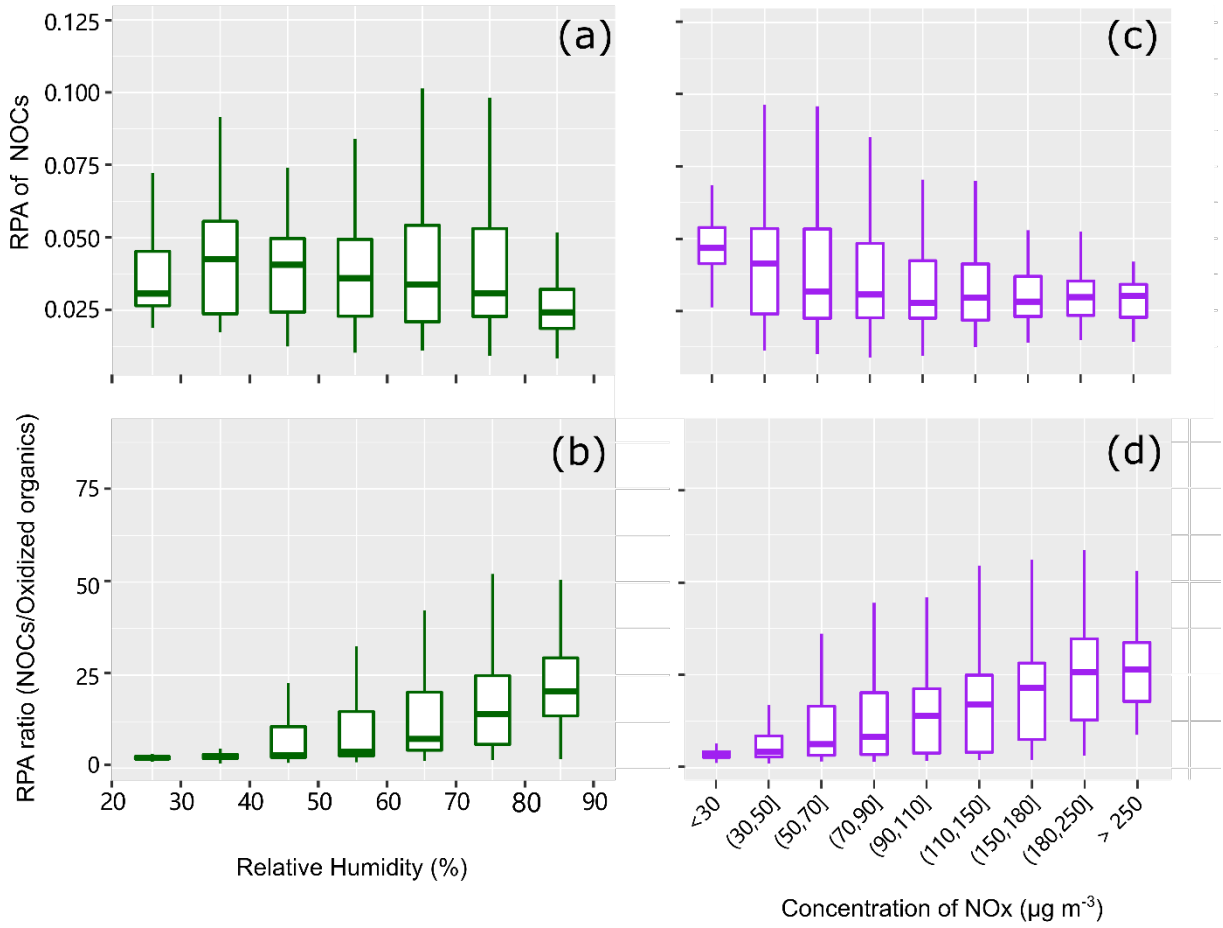
785



786

787

Fig. 5.



788

789

Fig. 6.